UDC 669.017:539.16

BLISTERING OF W, Ta AND W-Ta COATINGS UNDER THE INFLUENCE OF PARTICLES OF LOW-ENERGY HYDROGEN PLASMA

G.D. Tolstolutskaya, A.S. Kuprin, V.N. Voyevodin, A.V. Nikitin, V.D. Ovcharenko, V.A. Belous, R.L. Vasilenko, I.E. Kopanets
National Science Center "Kharkov Institute of Physics and Technology", Kharkov, Ukraine

The surface topography and deuterium retention in W, Ta and W-Ta coatings under the influence of low-energy deuterium plasma was studied. It was observed formation of blisters as dome and burst or delaminated structures. The W-Ta coatings showed improved characteristics: smaller sizes and density of blisters and a significantly lower thickness of the delaminated layer.

INTRODUCTION

Tungsten (W) will be used as a plasma-facing material (PFM) in the divertor region in ITER, and its use in future fusion devices is also very likely. The use of W as a PFM is attractive due to its excellent properties as high melting point, sputtering threshold or low tritium retention [1]. Tungsten shows also adequate corrosion resistance and the highest tensile strength of all metals at elevated temperatures [2]. The major issue associated with the presently available tungsten grades, in the context of structural applications, is their brittleness at low temperatures [3] which is worsened by irradiation [4]. Surface modifications might be problematic, because they can lead to degradation of heat conductivity. These modifications may further enhance erosion, which could be problematic because tungsten cannot be tolerated in the core plasma. An obvious way to solve this problem is to alloy W with other ductile refractory metals which also present low neutron activation [5] and recently refractory W composites were pointed as a promising alternative to pure W [6].

Alloying with Re, Mo or Ta can be used to modify the mechanical behavior of tungsten but limited property variation and precipitation of brittle secondary phases restrict this approach. Reinforcement of tungsten matrices with tungsten fibers has also been investigated [7] and the behavior of these composite systems seems, to a large extent, determined by the properties of the drawn tungsten fibers. For instance, potassium doped tungsten fibers enhance the strength and ductility of the material up to 2200 K [8]. However, the fabrication process by layer deposition of the tungsten matrices with tungsten fibers revealed weak bonding between the layers which leads to a composite cracking [7]. An alternative strategy to increase the toughness of W-based materials lies in dispersing ductile Ta particles or fibers in a W matrix [9–12].

Pure tantalum shows high toughness, low activation and high radiation resistance and, moreover, transmutes to W under high energy neutron irradiation. However, Ta is a scarce commodity and its extensive use as plasma facing material cannot be envisaged for large devices. A strategy to increase the fracture toughness of W-based materials for nuclear fusion applications lies on the development of W-Ta composites.

W-Ta alloys possess a higher corrosion resistance and better mechanical properties as compared to the pure tantalum. However, the obtaining of these alloys is complicated because of their high melting temperature [13]. It has been shown that nanostructure coatings from refractory metal may be obtained with the ion-plasma deposition methods [14]. Nanostructured metallic coatings, unlike the microcrystalline analogs, can have a higher hardness, strength and wear resistance. For example, magnetron nanocrystalline tantalum coatings have the hardness of ~ 11.6 GPa, and nanocrystalline and amorphous W-Ta coatings with tungsten concentration of 7.9…9.2 at.% have the hardness of 14.9 and 17.11 GPa, respectively [15].

The main changes in W-Ta composites under energetic ion bombardment could be followed by observing the induced effects in pure W and Ta plates irradiated at the same experimental conditions. The lower stiffness of Ta relatively to W results in the increase of the blistering mechanism in the Ta phase and this behavior could become magnified in the Ta component of composites due to water vapor production under D^+ bombardment. Hence, the enrichment of oxygen should be avoided during the alloying of the components. Blistering events and D retention highly decrease at lower incident energies and after D plasma bombardment the presence of a Ta component did not increase the fuel retention in the composite, which is promising for structural applications.

Lunyov, Kuprin et al. reported that W, Ta and W-Ta coatings deposited by argon ion sputtering of targets made from appropriate metals using the gas plasma source have higher mechanical properties as compared to the singlecomponent coatings [16].

The goal of this paper is the study of the surface topography of these W-Ta coatings and deuterium retention under the influence of particles of low-energy deuterium plasma and to compare with pure W and Ta plates exposed under the same irradiation conditions.

1. EXPERIMENTAL PROCEDURE

The design and principle of operation of the gas-plasma source (GPS) used for production of multicomponent coatings is described in detail in [16]. In the present paper a vacuum chamber comprises a GPS in the form of a tubular anode of 200 mm in diameter and 380 mm long with a tungsten hot cathode. Outside the anode there is a focusing coil, which generates a magnetic field of about 50 Oe. Experiments were carried using a filament current of a tungsten spiral of 100 A at a positive anode potential in the range of

+40…+50 V and argon pressure of ~ 0.5…0.8 Pa. The discharge current was 30…50 A. Sputtering targets were polycrystalline W and Ta plates onto which a negative potential of -500 V has been applied. The concentration of elements in the coatings was given by the ratio between the areas of tungsten and tantalum targets. The discharge-generated plasma was directed onto the target of the plasma-optical system. The anode-target distance was 50 mm. The ion-current density on the sputtering target was 10…20 mA/cm^2. Coatings were deposited on the substrates (10×20×1.5 mm) of stainless steel 18Cr10NiTi at a negative bias potential of -50 V. The substrate temperature during deposition did not exceed 500 °C. The coating deposition rate was of ~ 6 μm/h. The thickness of the coatings has been measured by the "shallow knifes" method using the microinterferometer MII-4.

Structure and properties of W, Ta and W-Ta coatings deposited by argon ion sputtering of targets were studied in [16]. It has been shown that W, Ta and W-Ta coating with tantalum content from 5 to 38% had a bcc structure. Introduction of the second component in the coating composition leads to the formation of a substitutional solid solution, in which the lattice parameter increases linearly with tantalum content increasing. Singlecomponent W and Ta coatings have a columnar structure with a strong axial structure and grain size of 29 and 25 nm, respectively.

The disk-shaped specimens have been irradiated at various temperatures with deuterium ions using a glow gas-discharge plasma electrodes at 1000 V, producing an ion flux of 10^{19} $D^+/(m^2 \cdot s)$. In this study we chose to use D in order to easily measure the depth dependence of the implanted and diffused hydrogen. While it is known that the mass difference of deuterium and protium isotopes of hydrogen can influence somewhat the thermodynamic and diffusional parameters somewhat via the well-known isotope effect. No significant differences in the development of the surface structure were previously observed between resulting from use of either deuterium or protium [17, 18].

The central portion of the specimen was irradiated through an aperture, providing an easily-observed boundary between irradiated and unirradiated regions. The maximum irradiation fluence was $2 \cdot 10^{25}$ D_2^+/m^2. The disk specimen was placed in a resistively-heated holder. The specimen temperature was continuously monitored using a thermocouple in the base of the specimen holder and was attached to the backside of specimen. The targets were exposed to high-flux deuterium plasmas at 300 K. The temperature was maintained to within ±2.5 K.

The kinetics of blister growth was monitored continuously during the irradiation using a video recorder. Investigations of surface microstructure were performed using a MMO-1600-AT metallographic microscope.

The implanted deuterium depth distribution was measured by means of the D(^{3}He, p)^{4}He nuclear reaction using the accelerator-measuring system ESU-2 [19]. The measurements were performed at room temperature using back scattering geometry. An analyzing beam of 300…1400 keV ^{3}He ions was used to examine the near-surface region of the specimen. The energy spectra of protons emitted by the nuclear reaction at different depths occurs at a rate proportional to the local deuterium concentration. Deuterium depth profiles were extracted from the obtained data using a software designated as Helen [20]. The depth resolution was determined to be ~ 200 nm and D depth profiles were determined up to a depth of 1.6 μm.

2. RESULTS AND DISCUSSION

Fig. 1 shows a SEM image of plasma-induced surface changes in a W coating bombarded at 300 K with 1 keV D_2^+ (0.5 keV/D) to $1 \cdot 10^{24}$ D_2^+/m^2. Blisters that formed on the plasma-exposed surface are clearly seen.

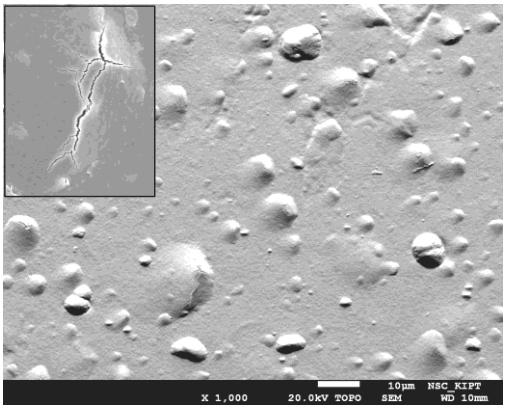

Fig. 1. SEM image of the tungsten coating bombarded with 1 keV D_2^+ to $1 \cdot 10^{24}$ D_2^+/m^2 at 300 K. Cracked blister (insert)

The mean size of the blisters ~ 3 μm and scattered from 0.5 to 10 μm. The blister number is $1.8 \cdot 10^{10}$ m^{-2}. Almost all blisters at the coating are asymmetric in shape and mostly cracked (see Fig. 1, insert).

Fig. 2 shows an SEM image of plasma-induced surface changes in tungsten foil (20 μm thickness) bombarded with 0.5 keV/D^+ to $1 \cdot 10^{24}$ D_2^+/m^2 at 300 K. The comparison of the shape of blisters shows that blisters at tungsten foil are domes. Blisters size and number in this case are 2 μm and $9 \cdot 10^{10}$ m^{-2}, respectively.

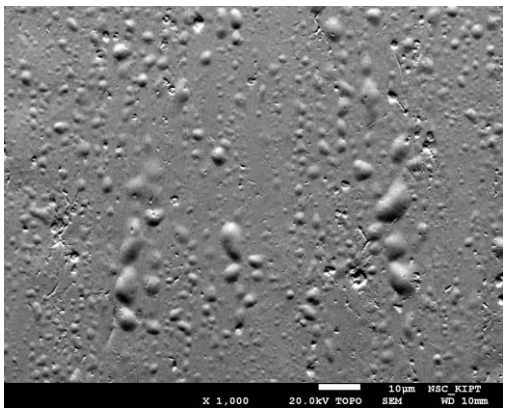

Fig. 2. SEM image of the tungsten foil bombarded with 1 keV D_2^+ to $1 \cdot 10^{24}$ D_2^+/m^2 at 300 K

The average size of blisters is comparable for the tungsten foil and coating, but in the coating the density of blisters is more than four times less.

Fig. 3 shows an SEM image of plasma-induced surface changes in tantalum coating bombarded with 0.5 keV/D^+ to $1 \cdot 10^{24}$ D_2^+/m^2.

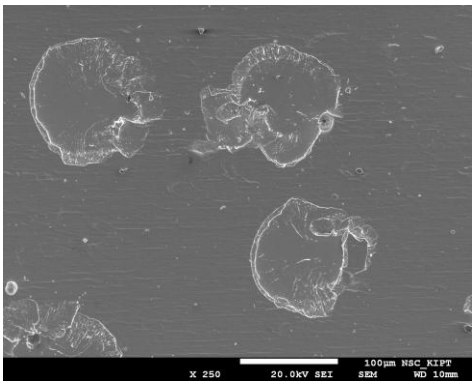

a

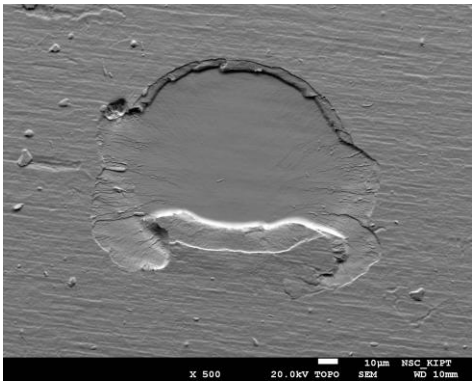

b

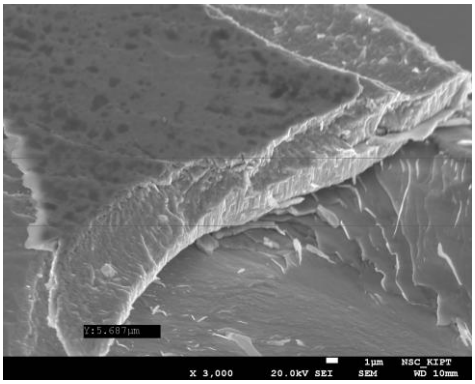

c

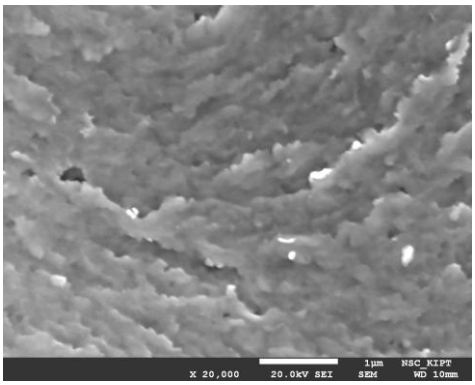

d

Fig. 3. SEM images of tantalum coating bombarded with 1 keV D_2^+ to $1 \cdot 10^{24}$ D_2^+/m^2 at 300 K: an overall image (a); morphology of delaminated blister (b); structure of the bursted layers (c); rupture surface(d)

Some large blisters are shown in Fig. 3,a. The blisters were burst and delaminated, meaning that they lost their caps (see Fig. 3,b). The critical size of the delaminated blisters is ~ 100 µm. The thickness of the bursted layers, having a columnar fiber structure, varies from 0.1 to 5 µm at radiation doses $1 \cdot 10^{24}$ D_2^+/m^2 (see Fig. 3,c). SEM image rupture surface is presented (see Fig. 3,d). As can be seen, the rupture occurs over the columnar grains.

When the dose was increased threefold, the destruction effect became stronger, up to the complete destruction of the coating in some places (Fig. 4,a). In the spectrum obtained by means of energy-dispersive X-ray spectroscopy the elements of the substrate – stainless steel 18Cr10NiTi were reliably fixed. Fig. 4,b shows an element of brittle rupture of a tantalum coating. As hydrogen accumulates, the blister cracks, and its lid breaks up into small pieces that are deposited on the surface of the sample.

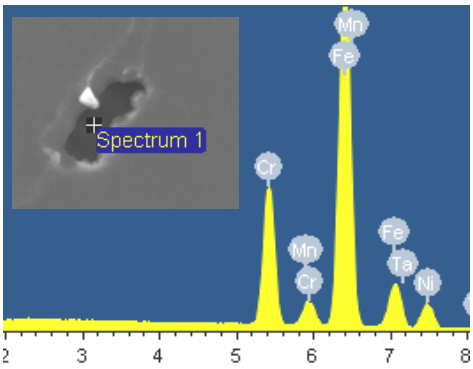

a

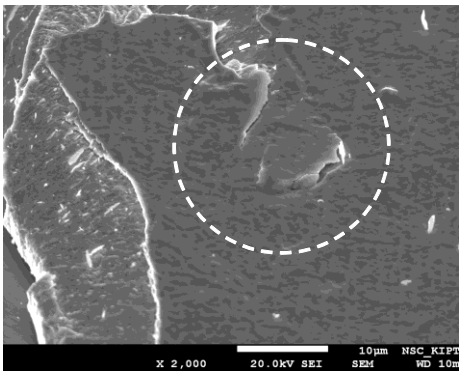

b

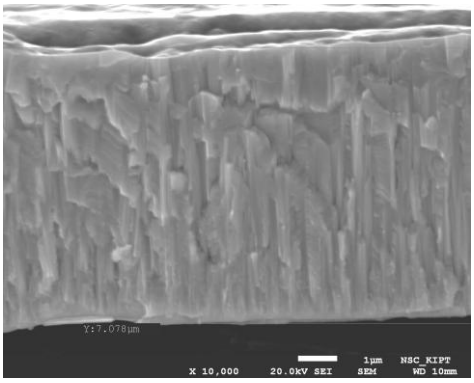

c

Fig. 4. SEM images of tantalum coating bombarded with 1 keV D_2^+ to $3 \cdot 10^{24}$ D_2^+/m^2 at 300 K. Destruction and composition of the substrate (a); element of brittle rupture (b); general view of the fracture surface (c)

The coating is damaged locally. Most of the volume of the coating retains its columnar structure up to doses $3 \cdot 10^{24}$ D_2^+/m^2 (see Fig. 4,c).

Fig. 5 shows an SEM image of plasma-induced surface changes in W-Ta coating (tantalum concentration 16 at.%) bombarded with 1 keV/D_2^+ to $1 \cdot 10^{24}$ D_2^+/m^2 at 300 K.

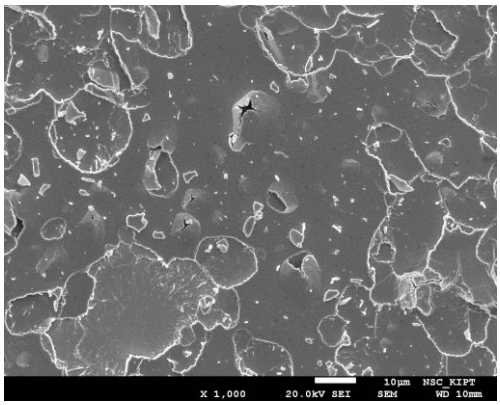

a

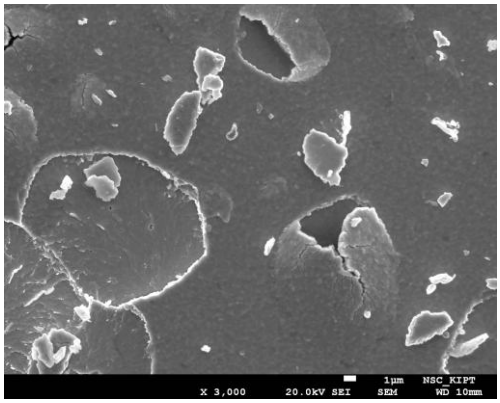

b

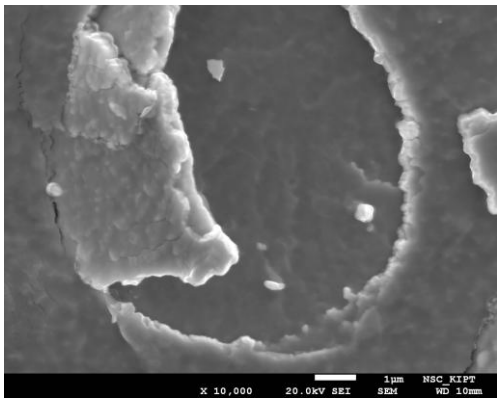

c

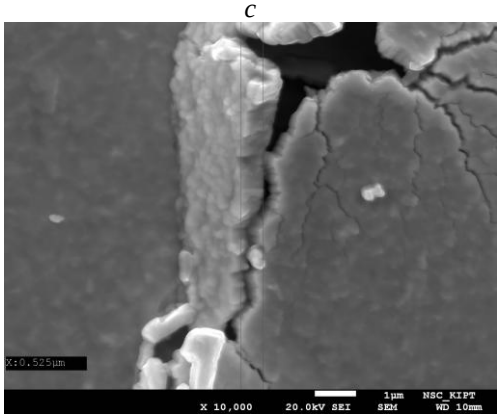

d

Fig. 5. SEM images of W-Ta coating bombarded at 300 K with 1 keV D_2^+ to $1 \cdot 10^{24}$ D_2^+/m^2 (a), different parts of the surface at different magnifications (b, c, d)

It can be seen that under the influence of particle fluxes from the low-energy hydrogen plasma the structures characteristic for the singlecomponent tungsten and tantalum coatings develop on the surface of sample (see Fig. 5,a). However, there are differences. "Classical" blisters size and number are ~ 3.5 μm and $6 \cdot 10^9$ m^{-2}, respectively. Many of them are destroyed more strongly (see Fig. 5,b,d). The bursted blisters have the critical size ~ 50 μm. The thickness of the bursted layers, having a columnar fiber structure, is less than one micron at radiation doses $1 \cdot 10^{24}$ D_2^+/m^2 (see Fig. 5,c,d). Small pieces of lids are deposited on the surface (see Fig. 5,b).

Thus, the W-Ta coating shows improved characteristics with respect to particle fluxes from the low-energy hydrogen plasma: smaller sizes and densities of blisters and a significantly lowered thickness of the delaminated layer.

In [21] was shown that oxygen remains in solid solution with Ta, leading to water vapour formation (D_2O) nearby the implanted depth of the Ta component under D irradiation, which results in additional gas pressure inside the blisters and in the magnification of the blistering mechanism. Mateus et al. shown that the slight oxidation during the milling of the metallic composites and the higher affinity of Ta to oxygen than of W leads to incorporation of oxygen in the Ta rich phase [21]. This oxygen contamination is probably not enough to form the oxide phase (Ta_2O_5), but a thin layer of this oxide could be formed during the preparation of metallographic samples. The enrichment of oxygen in Ta is responsible by the magnification of the blistering mechanism in the Ta phase in composites relatively to pure Ta samples.

The coatings deposited by ion sputtering of targets made from appropriate metals using the gas plasma source employed in this work are free from these oxide phases.

In addition to the degradation of the surface structure under the particle fluxes of deuterium plasma, an important task is to study the retention of hydrogen isotopes in the material of the first wall and the divertor of a thermonuclear reactor. Fig. 6 shows the depth profiles of deuterium retained in W coating exposed with 1 keV D_2^+ to $1 \cdot 10^{24}$ D_2^+/m^2 at 300 K.

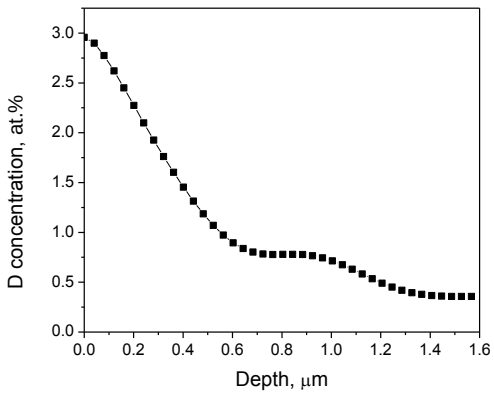

Fig. 6. Depth profiles of deuterium retained in W coating exposed with 1 keV D_2^+ to $1 \cdot 10^{24}$ D_2^+/m^2 at 300 K

In the W coating exposed to the D plasma, the deuterium depth profile is characterized by a near-surface concentration maximum of 3 at.% and, at depths above 0.4 μm, by a concentration of about 0.7 at.% slowly decreasing into the bulk (see Fig. 6).

Fig. 7 shows the depth profiles of deuterium retained in W-Ta coating exposed with 1 keV D_2^+ to $1 \cdot 10^{24}$ D_2^+/m^2 at 300 K.

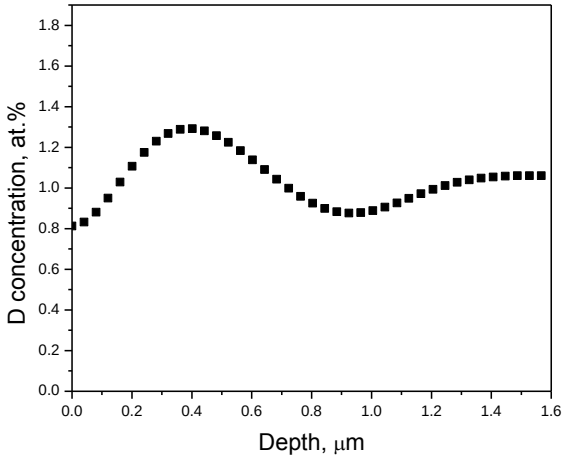

Fig. 7. Depth profiles of deuterium retained in W-Ta coating exposed to $1 \cdot 10^{24}$ D_2^+/m^2 at 300 K

In the W-Ta coating exposed under the same conditions, the deuterium depth profile is characterized by a concentration of about 1 at.% no decrease into the bulk up to a depth of 1.6 μm (see Fig. 7).

For W and W-Ta coatings exposed to the D plasma at dose $1 \cdot 10^{24}$ D_2^+/m^2, the deuterium retention in the 0…1.6 μm layer is the same and equals $1 \cdot 10^{21}$ m^{-2}.

For comparison, Fig. 8 shows the data for a massive foil of tantalum (90 μm thickness) rolled on stainless steel. The foil bombarded with 1 keV D_2^+ (0.5 keV/D) to dose $4 \cdot 10^{24}$ D_2^+/m^2 at 300 K.

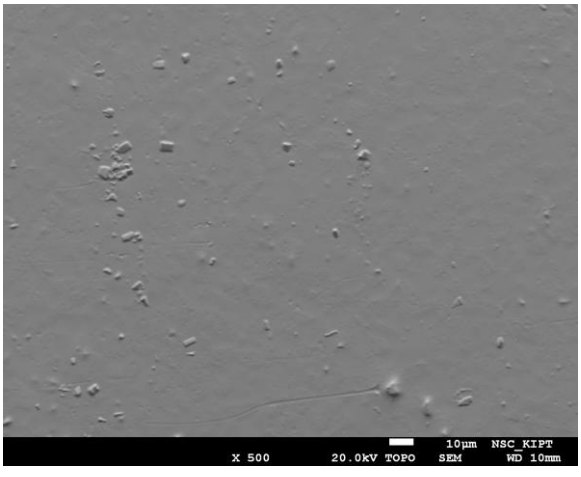

Fig. 8. SEM image of tantalum foil rolled on steel

No blister formation has been observed in Ta foil exposed at 300 K with 1 keV D_2^+ to $4 \cdot 10^{24}$ D_2^+/m^2 (see Fig. 8). In this case, the surface is subjected only to the sputtering process, which leads to the appearance of sufficiently large precipitates on the surface, weakly sputtered.

There are several conditions where blistering on W can be avoided. There is no blister formation at target temperatures of W ≥ 600 °C and after dual-energy irradiation. Also, on unpolished technical surfaces blisters do not form. We can suppose that in our case it is more likely the influence of unpolished surfaces.

The deuterium depth profile is characterized by a concentration of about 4 at.% weakly decrease into the bulk up to a depth of 1.6 μm (Fig. 9).

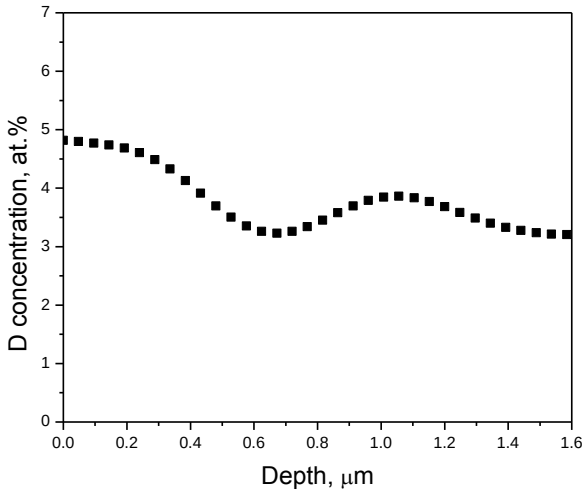

Fig. 9. Depth profiles of deuterium retained in Ta foil exposed with 1 keV D_2^+ to $4 \cdot 10^{24}$ D_2^+/m^2 at 300 K

Analysis of the literature showed the various discrepancies among works. In [22] an experimental study has been presented in which the properties of nanostructured tungsten films, deposited by PLD, are analyzed after high-flux deuterium plasma exposure (T_{max} = 520 K). An overview of the structure of the layers, blister and nanostructure formation, and deuterium retention is done. The pulsed laser deposition (PLD) layers withstand the plasma interaction maintaining their overall integrity. Nevertheless, abundant blister formation was observed on the PLD layers. The amount, distribution and shape depend on the W structure and layer thickness. For the high-density films, the growth seems to have preserved the grain structure as indicated by the observation of areas with clearly distinct nanostructures. The interfaces between these areas become fainter with decreasing film crystallinity and are completely gone for the amorphous-like films [22].

The deuterium retention has strongly increased for the PLD layers with respect to polycrystalline tungsten. Decrease of the layer density and crystalline order results in an increase in deuterium retention. The volumetric deuterium retention in columnar tungsten was found to be $7.4 \cdot 10^{26}$ m^{-3} which corresponds to 1.25 at.%. This is comparable to saturated values of deuterium retention in predamaged polycrystalline tungsten (at 0.45 dpa; 1.4 at.% ~ $8.8 \cdot 10^{26}$ m^{-3} [23]). The total retention in the pre-damaged sample was found to be $5.4 \cdot 10^{20}$ m^{-2}, the deuterium penetrated only 0.6 μm into the material. Thus, the penetration of deuterium into columnar tungsten is significantly quicker than penetration into pre-damaged tungsten. This makes sense since the crystallite size is typically ~ 2 nm and

the amorphous-like sample therefore contains many grain boundaries that presumably trap deuterium. In comparison, the volumetric retention of the amorphous-like layer with its density (only 60% of polycrystalline tungsten) amounts to 5.4 at.%.

Furthermore, the hydrogen retention in W-Ta composites is preferentially associated to the W component and composite production process.

The interaction of tokamak plasma with several materials considered for the plasma facing components of future fusion devices was studied in [24]. The samples were exposed to the edge plasma of the COMPASS tokamak which is a small-size device of the ITER-like diverted plasma shape with clear ohmic as well as NBI-assisted H-modes. These samples included mainly tungsten as the prime candidate and chromium steel as an alternative which suitability was to be assessed. For the experiments, thin coatings of tungsten, P92 steel and nickel on graphite substrates were prepared by arc discharge sputtering. The samples were exposed to hydrogen and deuterium plasma discharges in two modes: a) short exposure (several discharges) on a manipulator in the proximity of the separatrix, close to the central column, and b) long exposure (several months) at the central column, aligned with the other graphite tiles.

It has been shown that the surface layer enriched with hydrogen was similar to the unexposed samples. Deuterium enrichment was found only in the exposed samples, as a result of intake during deuterium discharges. The deuterium content was lower than that of hydrogen. The depth of the enriched layer was about 100 nm. On both pairs of exposed samples of the same type, i. e. tungsten and steel, the depth profiles of hydrogen and deuterium are very similar. The integral deuterium amount was extracted from ERDA depth profiles, but it should be taken into account that very low D concentration (less than 0.1 at.%) cannot be detected due to the ERDA limited accessible penetration depth and hydrogen signal background in ERDA spectrum. The deuterium contained in the surface layer observable by ERDA is comparable for W samples and estimated deuterium retention is ~ $6 \cdot 10^{19}$ atoms/m^2. For steel the integral amount of D in the observed layer was $4.5 \cdot 10^{19}$ atoms/m^2.

Deuterium (D) retention in polycrystalline tungsten (W) with copper (Cu) ion damage concurrently produced at elevated surface temperature is investigated [25]. An in situ heated stage held W samples at a controlled temperature up to 1243 K, which were subjected to displacement damage produced by 3.4 MeV Cu ions. D retention is subsequently explored by exposure of the W samples held at 383 K to a D_2 plasma ion fluence of 10^{24} D_2/m^2.

As remarked in Sakurada's paper [26], the various discrepancies among each work may show the sensitivity of defect recovery to dpa level. That is, the rates of vacancy-cluster and cluster-cluster formation competing with interstitial and free surface annihilation depend on the available concentration of these defects. For instance, the saturation of heavy ion induced defects as dpa approaches 0.3 that has not been observed for neutron damaged W.

Thus, the main trends in the retention of deuterium depend on the structure and layer thickness of coatings and defects produced by irradiation with plasma fluxes.

CONCLUSIONS

The surface topography of W, Ta and W-Ta coatings and deuterium retention under the influence of particles of low-energy deuterium plasma was studied.

It was observed formation of blisters as dome and burst or delaminated structures.

The W-Ta coating shows improved characteristics: smaller sizes and densities of blisters and a significantly lower thickness of the delaminated layer.

It is found, that the deuterium retention is the same and equals $1 \cdot 10^{21}$ m^{-2} and the concentration of deuterium is about 1 at.% for the W and W-Ta coatings exposed to the D plasma at dose $1 \cdot 10^{24}$ $D_2^+/m^{2.}$

The coatings deposited by argon ion sputtering of W and Ta targets using the gas plasma source employed in this work are free from oxygen enrichment.

REFERENCES

1. M. Ubeyli, S. Yalçm // *J. Fusion Energy*. 2006, v. 25, p. 197.
2. R.E. Nygren, R. Raffray, D. Whyte, M.A. Urickson, M. Baldwin, L.L. Snead. Making tungsten work // *J. Nucl. Mater*. 2011, v. 417, p. 451-456.
3. M.V. Korobova, N.V. Avramenko, A.G. Bogachev, N.V. Rozhkova, E. Osawa. Nanophase of water in nano-diamond gel // *J. Phys. Chem. C*. 2008, v. 111, p. 7330-7334.
4. I. Smid, M. Akiba, G. Vieider, L. Plooch. Development of tungsten armor and bonding cooper for plasma interactive components // *J. Nucl. Mater*. 1998, v. 258-263, p. 160-172.
5. M. Rieth et al. // *J. Nucl. Mater*. 2011, v. 417, p. 463.
6. Machlin, R.T. Begley, E.D. Weisert *// Proc. AIME Symp. on Refractory Metal Alloys, Metallurgy and Technology*, Plenum Press, New York, NY, 1968, p. 197.
7. H. Gieti, J. Riesch, J.W. Coenen, T. Hoschen, Ch. Linsmeier, R. Neu. Tensile deformation behavior of tungsten fiber-reinforced tungsten composite specimens in as fabricated state // *Fusion Eng. Des*. 2017, v. 122, p. 345-356.
8. J. Riesch, Y. Han, J. Almanstötter, J.W. Coenen, T. Hooschen, B. Jasper, P. Zhao, Ch. Linsmeier, R. Neu. Development of tungsten fiber-reinforced tungsten composites towards their use in DEMO-potassium doped tungsten wire // *Phys. Scr*. 2016, p. 014006.
9. V. Livramento, D. Nunes, J.B. Correia, P.A. Carvalho, R. Mateus, K. Hanada, N. Shohoji, H. Fernandes, C. Silva, E. Alves. Tungsten-tantalum composites for plasma facing components // *Materials for Energy 2010, ENMAT-2010, 4–8 July 2010*. Karlsruhe, Germany.
10. M. Dias, R. Mateus, N. Catarino, N. Franco, D. Nunes, J.B. Correia, P.A. Carvalho, K. Hanada, C. Sarbu, E. Alves. Synergistic helium and deuterium blistering in tungsten-tantalum composites // *J. Nucl. Mater*. 2013, v. 442, issue 1-3, p. 69-74.

11. M. Rieth et al. Recent progress in research on tungsten materials for nuclear fusion applications in Europe // *J. Nucl. Mater*. 2013, v. 432, p. 482-500.

12. L.H. Zhang, Y. Jiang, Q.F. Fang, T. Zhang, X.P. Wang, C.S. Liu. Toughness and microstructure of tungsten fiber net-reinforced tungsten composite produced by spark plasma sintering // *Mater. Sci. Eng. A*. 2016, v. 659, p. 29-36.

13. Young-Jun Lee, Tae-Hyuk Lee, Hayk H. Nersisyan, et al. Characterization of Ta-W alloy films deposited by molten salt Multi-Anode Reactive alloy Coating (MARC) method // *Int. Journal of Refractory Metals and Hard Materials.* 2015, v. 53, part A, p. 23-31.

14. J. Alami, P. Eklund, J.M. Andersson, M. Lattemann, E. Wallin, J. Bohlmark, P. Persson, U. Helmersson. Phase tailoring of Ta thin films by highly ionized pulsed magnetron sputtering // *Thin Solid Films*. 2007, v. 515, issue 7-8, p. 3434-3438.

15. C.L. Wang, M. Zhang, J.P. Chu, T.G. Nieh. Structures and nanoindentation properties of nanocrystalline and amorphous Ta-W thin films // *Scripta Materialia.* 2008, v. 58, p. 195-198.

16. V.M. Lunyov, A.S. Kuprin, V.D. Ovcharenko, V.A. Belous, A.N. Morozov, A.V. Ilchenko, G.N. Tolmachova, E.N. Reshetnyak, R.L. Vasilenko. Structure and properties of W, Ta and W-Ta coatings deposited with the use of a gas-plasma source // *Вопросы атомной науки и техники. Серия «Физика радиационных повреждений и радиационное материаловедение»*. 2016, №1(101), с. 140-144.

17. Г.Д. Толстолуцкая, А.В. Никитин, В.В. Ружицкий, Н.Д. Рыбальченко, Р.Л. Василенко, И.М. Короткова. Развитие трещин в ферритной стали при облучении водородной плазмой // *Вопросы атомной науки и техники. Серия «Физика радиационных повреждений и радиационное материаловедение»*. 2016, № 2(102), с. 25-32.

18. A.V. Nikitin, G.D. Tolstolutskaya, V.V. Ruzhytskyi, V.N. Voyevodin, I.E. Kopanets, S.A. Karpov, R.L. Vasilenko, F.A. Garner. Blister formation on 13Cr2MoNbVB ferritic-martensitic steel exposed to hydrogen plasma // *Journal of Nuclear Materials.* 2016, v. 478, p. 26-31.

19. Г.Д. Толстолуцкая, В.Н. Воеводин, И.М. Неклюдов, И.Е. Копанец. Метрологические характеристики методов неразрушающего контроля поверхностей твердых тел ионными пучками // *Труды XIX Национального научного симпозиума с международным участием «Метрология и метрологическое обеспечение 2009», с 10 сентября по 14 сентября 2009 г.* Болгария, Созополь, с. 173-179.

20. А.И. Жуков, В.Ф. Рыбалко, Г.Д. Толстолуцкая, И.Е. Копанец, Л.С. Верхоробин. Определение профиля залегания дейтерия в материалах по выходу продуктов ядерных реакций // *Вопросы атомной науки и техники. Серия «Физика радиационных повреждений и радиационное материаловедение»*. 1992, в. 1(58), 2(59), с. 133-135.

21. R. Mateus et al. Effects of helium and deuterium irradiation on SPS sintered W–Ta composites at different temperatures // *Journal of Nuclear Materials*. 2013, v. 442, p. S251-S255

22. M.H.J. 't Hoen, D. Dellasega, A. Pezzoli et al. Deuterium retention and surface modifications of nanocrystalline tungsten films exposed to high-flux plasma // *Journal of Nuclear Materials.* 2015, v. 463, p. 989-992.

23. Jirí Matejícek, Vladimír Weinzett, Anna Mackova, et al. Interaction of candidate plasma facing materials with tokamak plasma in COMPASS // *Journal of Nuclear Materials*. 2017, v. 493, p. 102-119.

24. R. Panek, J. Adamek, M. Aftanas, P. Bilkova, P. Boohm, F. Brochard, P. Cahyna, J. Cavalier, R. Dejarnac, M. Dimitrova, O. Grover, J. Harrison, P. Hacek, J. Havlicek, A. Havranek, J. Horacek, M. Hron, M. Imrisek, F. Janky, A. Kirk, M. Komm, K. Kovarik, J. Krbec, L. Kripner, T. Markovic, K. Mitosinkova, J. Mlynar, D. Naydenkova, M. Peterka, J. Seidl, J. Stoockel, E. _Stefanikova, M. Tomes, J. Urban, P. Vondracek, M. Varavin, J. Varju, V. Weinzettl, J. Zajac. Status of the COMPASS tokamak and characterization of the first H-Mode // *Plasma Phys. Control. Fusion*. 2016, v. 58, p. 014015.

25. M.J. Simmonds, Y.Q. Wang, J.L. Barton, et al. Reduced deuterium retention in simultaneously damaged and annealed tungsten // *Journal of Nuclear Materials.* 2017, v. 494, p. 67-71

26. S. Sakurada, K. Yuyama, Y. Uemura, H. Fujita, C. Hu, T. Toyama, N. Yoshida, T. Hinoki, S. Kondo, M. Shimada, D. Buchenauer, T. Chikada, Y. Oya. Annealing effects on deuterium retention behavior in damaged tungsten // *Nucl. Mater. Energy.* 2016, v. 9, p. 141-144..

Article received 04.10.2017

БЛИСТЕРИНГ W-, Ta- И W-Ta-ПОКРЫТИЙ ПРИ ВОЗДЕЙСТВИИ ПОТОКАМИ ЧАСТИЦ НИЗКОЭНЕРГЕТИЧНОЙ ВОДОРОДНОЙ ПЛАЗМЫ

Г.Д. Толстолуцкая, А.С. Куприн, В.Н. Воеводин, А.В. Никитин, В.Д. Овчаренко, В.А. Белоус, Р.Л. Василенко, И.Е. Копанец

Изучены изменение топографии поверхности покрытий W, Ta и W-Ta и накопление дейтерия под действием частиц низкоэнергетической дейтериевой плазмы. Наблюдалось образование блистеров куполообразной формы, отслаивание и шелушение. Покрытия W-Ta показали улучшенные характеристики: меньшие размеры и плотность блистеров и значительно уменьшенную толщину отслаиваемого слоя.

БЛІСТЕРІНГ W-, Ta- І W-Ta-ПОКРИТТІВ ПІД ДІЄЮ ПОТОКУ ЧАСТИНОК НИЗЬКОЕНЕРГЕТИЧНОЇ ВОДНЕВОЇ ПЛАЗМИ

Г.Д. Толстолуцька, А.С. Купрін, В.М. Воєводін, А.В. Нікітін, В.Д. Овчаренко, В.А. Білоус, Р.Л. Василенко, І.Є. Копанець

Вивчено зміну топографії поверхонь покриттів W, Ta і W-Ta і вміст дейтерію під дією частинок низькоенергетичної водневої плазми. Спостерігалося утворення блістерів куполоподібної форми, відшарування та лущення. Покриття W-Ta показали поліпшені характеристики: менші розміри і знижену густину блістерів і значно меншу товщину відшарованого шару.